

# An Optimal Control Approach to the Multi-Agent Persistent Monitoring Problem in Two-Dimensional Spaces

Xuchao Lin and Christos G. Cassandras

**Abstract**—We address the persistent monitoring problem in two-dimensional (2D) mission spaces where the objective is to control the movement of multiple cooperating agents to minimize an uncertainty metric. In a one-dimensional (1D) mission space, we have shown that the optimal solution is for each agent to move at maximal speed and switch direction at specific points, possibly waiting some time at each such point before switching. In a 2D mission space, such simple solutions can no longer be derived. An alternative is to optimally assign each agent a linear trajectory, motivated by the 1D analysis. We prove, however, that elliptical trajectories outperform linear ones. Therefore, we formulate a parametric optimization problem in which we seek to determine such trajectories. We show that the problem can be solved using Infinitesimal Perturbation Analysis (IPA) to obtain performance gradients on line and obtain a complete solution. Numerical examples are included to illustrate the main result and to compare our proposed scalable approach to trajectories obtained through off-line computationally intensive solutions.

## I. INTRODUCTION

Autonomous cooperating agents may be used to perform tasks such as coverage control [1], [2], surveillance [3] and environmental sampling [4]–[6]. *Persistent monitoring* arises in a large dynamically changing environment which cannot be fully covered by a stationary team of available agents. Thus, persistent monitoring differs from traditional coverage tasks due to the perpetual need to cover a changing environment, i.e., all areas of the mission space must be sensed infinitely often. The main challenge in designing control strategies in this case is in balancing the presence of agents in the changing environment so that it is covered over time optimally (in some well-defined sense) while still satisfying sensing and motion constraints.

Control and motion planning for agents performing persistent monitoring tasks have been studied in the literature, e.g., see [7]–[11]. In [12], we addressed the persistent monitoring problem by proposing an *optimal control* framework to drive a single agent so as to minimize a metric of uncertainty over the environment. This metric is a function of both space and time such that uncertainty at a point grows if it is not covered by any agent sensors. To model sensor coverage, we define a probability of detecting events at each point of the mission space by agent sensors. Thus, the uncertainty of the environment decreases with a rate proportional to the event detection probability, i.e., the

higher the sensing effectiveness is, the faster the uncertainty is reduced. This was extended to multiple cooperating agents in [13] and it was shown that the optimal control problem can be reduced to a *parametric* optimization problem. In particular, the optimal trajectory of each agent is to move at full speed until it reaches some switching point, dwell on the switching point for some time (possibly zero), and then switch directions. Thus, each agent’s optimal trajectory is fully described by a set of switching points  $\{\theta_1, \dots, \theta_K\}$  and associated waiting times at these points,  $\{w_1, \dots, w_K\}$ . This allowed us to make use of Infinitesimal Perturbation Analysis (IPA) [14] to determine gradients of the objective function with respect to these parameters and subsequently obtain optimal switching locations and waiting times that fully characterize an optimal solution. It also allowed us to exploit robustness properties of IPA to readily extend this solution approach to a *stochastic* uncertainty model.

In this paper, we address the same persistent monitoring problem in a 2D mission space. Using an analysis similar to the 1D case, we find that we can no longer identify a parametric representation of optimal agent trajectories. A complete solution requires a computationally intensive solution of a Two Point Boundary Value Problem (TPBVP) making any on-line solution to the problem infeasible. Motivated by the simple structure of the 1D problem, it has been suggested to assign each agent a linear trajectory for which the explicit 1D solution can be used. One could then reduce the problem to optimally carrying out this assignment. However, in a 2D space it is not obvious that a linear trajectory is a desirable choice. Indeed, a key contribution of this paper is to formally prove that an elliptical agent trajectory outperforms a linear one in terms of the uncertainty metric we are using. Motivated by this result, we formulate a 2D persistent monitoring problem as one of determining optimal elliptical trajectories for a given number of agents, noting that this includes the possibility that one or more agents share the same trajectory. We show that this problem can be explicitly solved using similar IPA techniques as in our 1D analysis. In particular, we use IPA to determine on line the gradient of the objective function with respect to the parameters that fully define each elliptical trajectory (center, orientation and length of the minor and major axes).

Section II formulates the optimal control problem for 2D mission spaces and Section III presents the standard solution approach. Section IV establishes our main result that elliptical trajectories outperform linear ones in terms of minimizing an uncertainty metric per unit area. In Section V we formulate and solve the problem of determining optimal

The authors’ work is supported in part by NSF under Grants EFRI-0735974 and CNS-1239021, by AFOSR under grant FA9550-12-1-0113, by ONR under grant N00014-09-1-1051, and by ARO under Grant W911NF-11-1-0227.

\* Division of Systems Engineering and Center for Information and Systems Engineering, Boston University; e-mail: {*mmxclin, cgc*}@bu.edu.

elliptical trajectories using a gradient-based algorithm driven by gradients evaluated through IPA. Section VI provides numerical results and section VII concludes the paper.

## II. PERSISTENT MONITORING PROBLEM FORMULATION

We consider  $N$  mobile agents in a 2D rectangular mission space  $\Omega \equiv [0, L_1] \times [0, L_2] \subset \mathbb{R}^2$ . Let the position of the agents at time  $t$  be  $s_n(t) = [s_n^x(t), s_n^y(t)]$  with  $s_n^x(t) \in [0, L_1]$  and  $s_n^y(t) \in [0, L_2]$ ,  $n = 1, \dots, N$ , following the dynamics:

$$\dot{s}_n^x(t) = u_n(t) \cos \theta_n(t), \quad \dot{s}_n^y(t) = u_n(t) \sin \theta_n(t) \quad (1)$$

where  $u_n(t)$  is the scalar speed of the  $n$ th agent and  $\theta_n(t)$  is the angle relative to the positive direction that satisfies  $0 \leq \theta_n(t) < 2\pi$ . Thus, we assume that each agent controls its orientation and speed. Without loss of generality, after some rescaling of the size of the mission space, we further assume that the speed is constrained by  $0 \leq u_n(t) \leq 1$ ,  $n = 1, \dots, N$ . Each agent is represented as a particle in the 2D space, thus we ignore the case of two or more agents colliding with each other.

We associate with every point  $[x, y] \in \Omega$  a function  $p_n(x, y, s_n)$  that measures the probability that an event at location  $[x, y]$  is detected by agent  $n$ . We also assume that  $p_n(x, y, s_n) = 1$  if  $[x, y] = s_n$ , and that  $p_n(x, y, s_n)$  is monotonically nonincreasing in the Euclidean distance  $D(x, y, s_n) \equiv \|[x, y] - s_n\|$  between  $[x, y]$  and  $s_n$ , thus capturing the reduced effectiveness of a sensor over its range which we consider to be finite and denoted by  $r_n$  (this is the same as the concept of “sensor footprint” commonly used in the robotics literature.) Therefore, we set  $p_n(x, y, s_n) = 0$  when  $D(x, y, s_n) > r_n$ . Our analysis is not affected by the precise sensing model  $p_n(x, y, s_n)$ , but we mention here as an example the linear decay model used in [13]:

$$p_n(x, y, s_n) = \begin{cases} 1 - \frac{D(x, y, s_n)}{r_n}, & \text{if } D(x, y, s_n) \leq r_n \\ 0, & \text{if } D(x, y, s_n) > r_n \end{cases} \quad (2)$$

Next, consider a set of points  $\{[\alpha_i, \beta_i], i = 1, \dots, M\}$ ,  $[\alpha_i, \beta_i] \in \Omega$ , and associate a time-varying measure of uncertainty with each point  $[\alpha_i, \beta_i]$ , which we denote by  $R_i(t)$ . The set of points  $\{[\alpha_1, \beta_1], \dots, [\alpha_M, \beta_M]\}$  may be selected to contain specific “points of interest” in the environment, or simply to sample points in the mission space. Alternatively, we may consider a partition of  $\Omega$  into  $M$  rectangles denoted by  $\Omega_i$  whose center points are  $[\alpha_i, \beta_i]$ . We can then set  $p_n(x, y, s_n(t)) = p_n(\alpha_i, \beta_i, s_n(t))$  for all  $\{[x, y] | [x, y] \in \Omega_i, [\alpha_i, \beta_i] \in \Omega_i\}$ , i.e., for all  $[x, y]$  in the rectangle  $\Omega_i$  that  $[\alpha_i, \beta_i]$  belongs to. Therefore, the joint probability of detecting an event at location  $[\alpha_i, \beta_i]$  by all the  $N$  agents (assuming detection independence) is

$$P_i(\mathbf{s}(t)) = 1 - \prod_{n=1}^N [1 - p_n(\alpha_i, \beta_i, s_n(t))]$$

where we set  $\mathbf{s}(t) = [s_1(t), \dots, s_N(t)]^T$ . Similar to the 1D analysis in [13], we define uncertainty functions  $R_i(t)$  associated with the rectangles  $\Omega_i$ ,  $i = 1, \dots, M$ , so that they have the following properties: (i)  $R_i(t)$  increases with a prespecified rate  $A_i$  if  $P_i(\mathbf{s}(t)) = 0$ , (ii)  $R_i(t)$  decreases with

a fixed rate  $B$  if  $P_i(\mathbf{s}(t)) = 1$  and (iii)  $R_i(t) \geq 0$  for all  $t$ . It is then natural to model uncertainty so that its decrease is proportional to the probability of detection. In particular, we model the dynamics of  $R_i(t)$ ,  $i = 1, \dots, M$ , as follows:

$$\dot{R}_i(t) = \begin{cases} 0 & \text{if } R_i(t) = 0, A_i \leq BP_i(\mathbf{s}(t)) \\ A_i - BP_i(\mathbf{s}(t)) & \text{otherwise} \end{cases} \quad (3)$$

where we assume that initial conditions  $R_i(0)$ ,  $i = 1, \dots, M$ , are given and that  $B > A_i > 0$  for all  $i = 1, \dots, M$ ; thus, the uncertainty strictly decreases when there is perfect sensing  $P_i(\mathbf{s}(t)) = 1$ .

As described in [12], persistent monitoring can be viewed as a polling system, with each rectangle  $\Omega_i$  associated with a “virtual queue” where uncertainty accumulates with inflow rate  $A_i$ . The service rate of this queue is time-varying and given by  $BP_i(\mathbf{s}(t))$ , controllable through all agent positions at time  $t$ .

The goal of the optimal persistent monitoring problem we consider is to control through  $u_n(t)$ ,  $\theta_n(t)$  in (1) the movement of the  $N$  agents so that the cumulative uncertainty over all sensing points  $\{[\alpha_1, \beta_1], \dots, [\alpha_M, \beta_M]\}$  is minimized over a fixed time horizon  $T$ . Thus, setting  $\mathbf{u}(t) = [u_1(t), \dots, u_N(t)]$  and  $\boldsymbol{\theta}(t) = [\theta_1(t), \dots, \theta_N(t)]$  we aim to solve the following optimal control problem **P1**:

$$\min_{\mathbf{u}(t), \boldsymbol{\theta}(t)} J = \int_0^T \sum_{i=1}^M R_i(t) dt \quad (4)$$

subject to the agent dynamics (1), uncertainty dynamics (3), control constraint  $0 \leq u_n(t) \leq 1$ ,  $0 \leq \theta_n(t) \leq 2\pi$ ,  $t \in [0, T]$ , and state constraints  $s_n(t) \in \Omega$  for all  $t \in [0, T]$ ,  $n = 1, \dots, N$ .

## III. OPTIMAL CONTROL SOLUTION

We first characterize the optimal control solution of problem **P1**. We define the state vector  $\mathbf{x}(t) = [s_1^x(t), s_1^y(t), \dots, s_N^x(t), s_N^y(t), R_1(t), \dots, R_M(t)]^T$  and the associated costate vector  $\boldsymbol{\lambda}(t) = [\mu_1^x(t), \mu_1^y(t), \dots, \mu_N^x(t), \mu_N^y(t), \lambda_1(t), \dots, \lambda_M(t)]^T$ . In view of the discontinuity in the dynamics of  $R_i(t)$  in (3), the optimal state trajectory may contain a boundary arc when  $R_i(t) = 0$  for any  $i$ ; otherwise, the state evolves in an interior arc. We first analyze the system operating in such an interior arc and omit the state constraint  $s_n(t) \in \Omega$ ,  $n = 1, \dots, N$ ,  $t \in [0, T]$ . Using (1) and (3), the Hamiltonian is

$$H = \sum_i R_i(t) + \sum_i \lambda_i \dot{R}_i(t) + \sum_n \mu_n^x(t) u_n(t) \cos \theta_n(t) + \sum_n \mu_n^y(t) u_n(t) \sin \theta_n(t) \quad (5)$$

and the costate equations  $\dot{\boldsymbol{\lambda}} = -\frac{\partial H}{\partial \mathbf{x}}$  are

$$\dot{\lambda}_i(t) = -\frac{\partial H}{\partial R_i} = -1 \quad (6)$$

$$\begin{aligned}\dot{\mu}_n^x(t) &= -\frac{\partial H}{\partial s_n^x} = -\sum_i \frac{\partial}{\partial s_n^x} \lambda_i \dot{R}_i(t) \\ &= -\sum_{(\alpha_i, \beta_i) \in \mathcal{R}(s_n)} \frac{B\lambda_i}{r_n D(\alpha_i, \beta_i, s_n(t))} (s_n^x - \alpha_i)\end{aligned}\quad (7)$$

$$\begin{aligned}\dot{\mu}_n^y(t) &= -\frac{\partial H}{\partial s_n^y} = -\sum_i \frac{\partial}{\partial s_n^y} \lambda_i \dot{R}_i(t) \\ &= -\sum_{(\alpha_i, \beta_i) \in \mathcal{R}(s_n)} \frac{B\lambda_i}{r_n D(\alpha_i, \beta_i, s_n(t))} (s_n^y - \beta_i)\end{aligned}\quad (8)$$

where  $\mathcal{R}(s_n) \equiv \{[\alpha_i, \beta_i] \mid D(\alpha_i, \beta_i, s_n) \leq r_n, R_i > 0\}$  identifies all points  $[\alpha_i, \beta_i]$  within the sensing range of the agent using the model in (2). Since we impose no terminal state constraints, the boundary conditions are  $\lambda_i(T) = 0, i = 1, \dots, M$  and  $\mu_n^x(T) = 0, \mu_n^y(T) = 0, n = 1, \dots, N$ . The implication of (6) with  $\lambda_i(T) = 0$  is that  $\lambda_i(t) = T - t$  for all  $t \in [0, T], i = 1, \dots, M$  and that  $\lambda_i(t)$  is monotonically decreasing starting with  $\lambda_i(0) = T$ . However, this is only true if the entire optimal trajectory is an interior arc, i.e., all  $R_i(t) \geq 0$  constraints for all  $i = 1, \dots, M$  remain inactive. We have shown in [12] that  $\lambda_i(t) \geq 0, i = 1, \dots, M, t \in [0, T]$  with equality holding only if  $t = T$ , or  $t = t_0^-$  with  $R_i(t_0) = 0, R_i(t') > 0$ , where  $t' \in [t_0 - \delta, t_0), \delta > 0$ . Although this argument holds for the 1D problem formulation, the proof can be directly extended to this 2D environment. However, the actual evaluation of the full costate vector over the interval  $[0, T]$  requires solving (7) and (8), which in turn involves the determination of all points where the state variables  $R_i(t)$  reach their minimum feasible values  $R_i(t) = 0, i = 1, \dots, M$ . This generally involves the solution of a TPBVP.

From (5), after some algebraic operations and combining the trigonometric function terms, we obtain

$$\begin{aligned}H &= \sum_i R_i(t) + \sum_i \lambda_i \dot{R}_i(t) \\ &+ \sum_n \operatorname{sgn}(\mu_n^y) u_n(t) \frac{\sin(\theta_n(t) + \varphi_n(t))}{\sqrt{(\mu_n^x(t))^2 + (\mu_n^y(t))^2}}\end{aligned}\quad (9)$$

where  $\operatorname{sgn}(\cdot)$  is the sign function and  $\varphi_n(t)$  is defined so that  $\tan \varphi_n(t) = \frac{\mu_n^x(t)}{\mu_n^y(t)}$ . Applying the Pontryagin minimum principle to (9) with  $u_n^*(t), \theta_n^*(t), t \in [0, T]$ , denoting an optimal control, we have

$$H(\mathbf{x}^*, \lambda^*, \mathbf{u}^*, \theta^*) = \min_{\mathbf{u} \in [0, 1], \theta \in [0, 2\pi]} H(\mathbf{x}, \lambda, \mathbf{u}, \theta)$$

and it is immediately obvious that it is necessary for an optimal control to satisfy  $u_n^*(t) = 1$  and

$$\begin{cases} \theta_n^*(t) = \frac{\pi}{2} - \varphi_n(t), & \text{if } \mu_n^y(t) < 0 \\ \theta_n^*(t) = \frac{3\pi}{2} - \varphi_n(t), & \text{if } \mu_n^y(t) > 0 \end{cases}\quad (10)$$

Returning to the Hamiltonian in (5), the optimal heading  $\theta_n^*(t)$  can be obtained by requiring  $\frac{\partial H^*}{\partial \theta_n^*} = 0$ :

$$\frac{\partial H}{\partial \theta_n} = -\mu_n^x(t) u(t) \sin \theta_n(t) + \mu_n^y(t) u(t) \cos \theta_n(t) = 0$$

which gives  $\tan \theta_n^*(t) = \frac{\mu_n^y(t)}{\mu_n^x(t)}$ .

Since we have shown that  $u_n^*(t) = 1, n = 1, \dots, N$ , we are only left with the task of determining  $\theta_n^*(t), n = 1, \dots, N$ . This can be accomplished by solving a standard TPBVP problem involving forward and backward integrations of the state and costate equations to evaluate  $\frac{\partial H}{\partial \theta_n}$  after each such iteration and using a gradient descent approach until the objective function converges to a (local) minimum. Clearly, this is a computationally intensive process which scales poorly with the number of agents and the size of the mission space. In addition, it requires discretizing the mission time  $T$  and calculating every control at each time step which adds to the computational complexity.

#### IV. LINEAR VS ELLIPTICAL AGENT TRAJECTORIES

Given the complexity of the TPBVP required to obtain an optimal solution of problem **P1**, we seek alternative approaches which may be suboptimal but are tractable and scalable. The first such effort is motivated by the results obtained in our 1D analysis, where we found that on a mission space defined by a line segment  $[0, L]$  the optimal trajectory for each agent is to move at full speed until it reaches some switching point, dwell on the switching point for some time (possibly zero), and then switch directions. Thus, each agent's optimal trajectory is fully described by a set of switching points  $\{\theta_1, \dots, \theta_K\}$  and associated waiting times at these points,  $\{w_1, \dots, w_K\}$ . The values of these parameters can then be efficiently determined using a gradient-based algorithm with Infinitesimal Perturbation Analysis (IPA) to evaluate the objective function gradient as shown in [13].

Thus, a reasonable approach that has been suggested is to assign each agent a linear trajectory. The 2D persistent monitoring problem would then be formulated as consisting of the following tasks: (i) finding  $N$  linear trajectories in terms of their length and exact location in  $\Omega$ , noting that one or more agents may share one of these trajectories, and (ii) controlling the motion of each agent on its trajectory. Task (ii) is a direct application of the 1D persistent monitoring problem solution, leaving only task (i) to be addressed. However, there is no reason to believe that a linear trajectory is a good choice in a 2D setting. A broader choice is provided by elliptical trajectories which in fact encompass linear ones when the minor axis of the ellipse becomes zero. Thus, we first proceed with a comparison of these two types of trajectories. The main result of this section is to formally show that an elliptical trajectory outperforms a linear one using the average uncertainty metric in (4) as the basis for such comparison.

To simplify notation, let  $\omega = [x, y] \in \mathbb{R}^2$  and, for a single agent, define

$$\Omega = \{\omega \in \mathbb{R}^2 \mid \exists t \in [0, T] \text{ such that } Bp(\omega, s(t)) > A(\omega)\}\quad (11)$$

Note that  $\Omega$  above defines the *effective coverage region* for the agent, i.e., the region where the uncertainty corresponding to  $R(\omega, t)$  with the dynamics in (3) can be strictly reduced given the sensing capacity of the agent determined through  $B$  and  $p(\omega, s)$ . Clearly,  $\Omega$  depends on the values

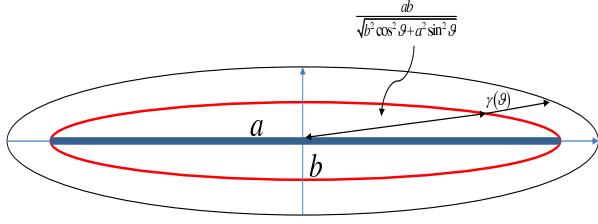


Fig. 1. The red ellipse represents the agent trajectory. The area defined by the black curve is the agent's effective coverage area.  $\frac{ab}{\sqrt{b^2 \cos^2(\vartheta) + a^2 \sin^2(\vartheta)}} + \gamma(\vartheta)$  is the distance between the ellipse center and the coverage area boundary for a given  $\vartheta$ .

of  $s(t)$  which are dependent on the agent trajectory. Let us define an elliptical trajectory so that the agent position  $s(t) = [s^x(t), s^y(t)]$  follows the general parametric form of an ellipse:

$$\begin{cases} s^x(t) = X + a \cos \rho(t) \cos \varphi - b \sin \rho(t) \sin \varphi \\ s^y(t) = Y + a \cos \rho(t) \sin \varphi + b \sin \rho(t) \cos \varphi \end{cases} \quad (12)$$

where  $[X, Y]$  is the center of the ellipse,  $a, b$  are its major and minor axis respectively,  $\varphi \in [0, \pi)$  is the ellipse orientation (the angle between the  $x$  axis and the major ellipse axis) and  $\rho(t) \in [0, 2\pi)$  is the eccentric anomaly of the ellipse. Assuming the agent moves with constant maximal speed 1 on this trajectory, we have  $(\dot{s}^x)^2 + (\dot{s}^y)^2 = 1$ , which gives  $\dot{\rho}(t) = [(a \sin \rho(t) \cos \varphi + b \cos \rho(t) \sin \varphi)^2 + (a \sin \rho(t) \sin \varphi - b \cos \rho(t) \cos \varphi)^2]^{-1/2}$ . In order to make a fair comparison between a linear and an elliptical trajectory, we normalize the objective function in (4) with respect to the coverage area in (11) and consider all points in  $\Omega$  (rather than discretizing it or limiting ourselves to a finite set of sampling points). Thus, we define:

$$J(b) = \frac{1}{\Psi_\Omega} \int_0^T \int_\Omega R(\omega, t) d\omega dt \quad (13)$$

where  $\Psi_\Omega = \int_\Omega d\omega$  is the area of the effective coverage region. Note that we view this normalized metric as a function of  $b \geq 0$ , so that when  $b = 0$  we obtain the uncertainty corresponding to a linear trajectory. For simplicity, the trajectory is selected so that  $[X, Y]$  coincides with the origin and  $\varphi = 0$ , as illustrated in Fig. 1 with the major axis  $a$  assumed fixed. Regarding the range of  $b$ , we will only be interested in values which are limited to a neighborhood near zero which we will denote by  $\mathcal{B}$ . Given  $a$ , this set dictates the values that  $s(t) \in \Omega$  is allowed to take. Finally, we make the following assumptions:

**Assumption 1:**  $p(\omega, s) \equiv p(D(\omega, s))$  is a continuous function of  $D(\omega, s) \equiv \|\omega - s\|$ .

**Assumption 2:** Let  $\omega, \omega'$  be symmetric points in  $\Omega$  with respect to the center point of the ellipse. Then,  $A(\omega) = A(\omega')$ .

The first assumption simply requires that the sensing range of an agent is continuous and the second that all points in  $\Omega$  are treated uniformly with respect to an elliptical trajectory centered in this region. The following result establishes the fact that an elliptical trajectory with some  $b > 0$  can achieve

a lower cost than a linear trajectory (i.e.,  $b = 0$ ) in terms of a long-term average uncertainty per unit area.

*Proposition IV.1:* Under Assumptions 1-2 and  $b \in \mathcal{B}$ ,

$$\lim_{T \rightarrow \infty, b \rightarrow 0} \frac{\partial J(b)}{\partial b} < 0$$

i.e., switching from a linear to an elliptical trajectory reduces the cost in (13).

**Proof.** Since a linear trajectory is the limit of an elliptical one (with the major axis kept fixed) as the minor axis reaches  $b = 0$ , our proof is based on perturbing the minor axis  $b$  away from 0 and showing that we can then achieve a lower average cost  $J$  in (13), as long as this is measured over a sufficiently long time interval.

Obviously, the effective coverage area  $\Psi_\Omega$  depends on the agent's trajectory and, in particular, on the minor axis length  $b$ . From the definition of  $\Omega$  in (11), note that  $\Psi_\Omega$  monotonically increases in  $b \in \mathcal{B}$ , i.e.,  $\frac{\partial \Psi_\Omega}{\partial b} > 0$  and it immediately follows that:

$$\frac{\partial}{\partial b} \left( \frac{1}{\Psi_\Omega} \right) = - \frac{\partial \Psi_\Omega}{\partial b} \frac{1}{\Psi_\Omega^2} < 0 \quad (14)$$

We now rewrite the area integral in (13) in a polar coordinate system with  $\omega = (\xi, \vartheta) \in \mathbb{R}^2$ , where  $\xi$  is the polar radius and  $\vartheta$  is the polar angle:

$$J(b) = \frac{1}{\Psi_\Omega} \int_0^T \int_0^{2\pi} \int_0^{G(a,b,\vartheta)+\gamma(\vartheta)} R(\xi, \vartheta, t) \xi d\xi d\vartheta dt \quad (15)$$

where

$$G(a, b, \vartheta) = \frac{ab}{\sqrt{b^2 \cos^2(\vartheta) + a^2 \sin^2(\vartheta)}} \quad (16)$$

is the ellipse equation in the polar coordinate system and  $\gamma(\vartheta)$  is defined for any  $(\xi, \vartheta) \in \mathbb{R}^2$  as

$$\gamma(\vartheta) = \sup_{\xi} \{ Bp(\xi, \vartheta, s(t)) > A(\xi, \vartheta) \} - G(a, b, \vartheta)$$

where  $\sup_{\xi} \{ Bp(\xi, \vartheta, s(t)) > A(\xi, \vartheta) \}$  is the distance between the ellipse center and the furthest point  $(\xi, \vartheta)$ , for any given  $\vartheta$ , that can be effectively covered by the agent on the ellipse. Taking partial derivatives in (15) with respect to  $b$ , we get

$$\begin{aligned} \frac{\partial J}{\partial b} &= - \frac{\partial \Psi_\Omega}{\partial b} \frac{1}{\Psi_\Omega^2} \int_0^T \int_\Omega R(\omega, t) d\omega dt \\ &+ \frac{1}{\Psi_\Omega} \int_0^T \int_0^{2\pi} [R(G(a, b, \vartheta) + \gamma(\vartheta), \vartheta, t) \\ &\cdot (G(a, b, \vartheta) + \gamma(\vartheta)) \cdot \frac{\partial G(a, b, \vartheta)}{\partial b} \\ &+ \int_0^{G(a, b, \vartheta) + \gamma(\vartheta)} \frac{\partial R(\xi, \vartheta, t)}{\partial b} \xi d\xi] d\vartheta dt \end{aligned} \quad (17)$$

Recall that our objective is to show that when we perturb a linear trajectory into an elliptical one by increasing  $b$  from 0 to some small  $b_\epsilon > 0$  we can achieve a lower cost. Thus, we aim to show that  $\frac{\partial J}{\partial b}|_{b \rightarrow 0} < 0$ . From (14), the first term of (17) is negative, therefore, we only need to show that the second

term is non-positive when  $b \rightarrow 0$ . By the definition (16), observe that when  $b \rightarrow 0$ ,  $G(a, b, \vartheta) \rightarrow 0$ , and  $\frac{\partial G(a, b, \vartheta)}{\partial b}|_{b \rightarrow 0} = \frac{1}{\sin \vartheta}$ . Thus, the double integral of the second term of (17) becomes

$$\int_0^T \int_0^{2\pi} \left[ \frac{\gamma(\vartheta)}{\sin \vartheta} R(\gamma(\vartheta), \vartheta, t) + \int_0^{\gamma(\vartheta)} \frac{\partial R(\xi, \vartheta, t)}{\partial b} \xi d\xi \right] d\vartheta dt \quad (18)$$

By Assumption 2,  $A(\omega) = A(\omega')$ , where  $\omega$  and  $\omega'$  are symmetric with respect to the center point of the ellipse, thus  $A(\xi, \vartheta) = A(\xi, \vartheta + \pi)$ . Then, for any uncertainty value  $R(\gamma(\vartheta), \vartheta, t)$ , we can find  $R(\gamma(\vartheta + \pi), \vartheta + \pi, t)$  which is symmetric to it with respect to the center point of the ellipse and note that  $\gamma(\vartheta) = \gamma(\vartheta + \pi)$ . From the perspective of the point  $(\gamma(\vartheta), \vartheta)$ , the agent movement observed with an initial position  $\rho(0) = \eta$  (following the dynamics in (IV)) is the same as the movement observed from  $(\gamma(\vartheta + \pi), \vartheta + \pi)$  if the agent starts from  $\rho(0) = \eta + \pi$  when  $T \rightarrow \infty$ , since the cost in (13) is independent of initial conditions as  $T \rightarrow \infty$ . Thus  $R(\gamma(\vartheta), \vartheta, t) = R(\gamma(\vartheta + \pi), \vartheta + \pi, t)$ . Since, in addition,  $\sin \vartheta = -\sin(\vartheta + \pi)$ , we have  $\gamma(\vartheta) \frac{R(\gamma(\vartheta), \vartheta, t)}{\sin \vartheta} = -\gamma(\vartheta + \pi) \frac{R(\gamma(\vartheta + \pi), \vartheta + \pi, t)}{\sin(\vartheta + \pi)}$  and it follows that

$$\lim_{T \rightarrow \infty, b \rightarrow 0} \int_0^T \int_0^{2\pi} \frac{\gamma(\vartheta)}{\sin \vartheta} R(\gamma(\vartheta), \vartheta, t) d\vartheta dt = 0 \quad (19)$$

We now turn our attention to the last integral of (17). Two cases need to be considered here: (i) if  $\exists t'$  such that  $R(\xi, \vartheta, t') = 0$  for  $t' \in (0, t)$ , then let

$$\tau_f(t) = \sup_{\tau \leq t} \{ \tau : R(\xi, \vartheta, \tau) = 0 \} \quad (20)$$

If  $\tau_f(t) < t$ , then  $R(\xi, \vartheta, \tau) > 0$  for all  $\tau \in [\tau_f(t), t)$  and  $\tau_f(t)$  is the last time instant prior to  $t$  when  $R(\xi, \vartheta, \tau) = 0$ . We can then write  $R(\xi, \vartheta, t) = \int_{\tau_f(t)}^t \dot{R}(\xi, \vartheta, \delta) d\delta$ . Therefore,

$$\begin{aligned} \frac{\partial R(\xi, \vartheta, t)}{\partial b} &= \frac{\partial t}{\partial b} \dot{R}(\xi, \vartheta, t) - \frac{\partial \tau_f(t)}{\partial b} \dot{R}(\xi, \vartheta, \tau_f(t)) \\ &+ \int_{\tau_f(t)}^t \frac{\partial \dot{R}(\xi, \vartheta, \delta)}{\partial b} d\delta \end{aligned} \quad (21)$$

Clearly,  $\frac{\partial t}{\partial b} = 0$  and since  $\tau_f(t)$  is a time instant when  $R(\xi, \vartheta, t)$  leaves  $R(\xi, \vartheta, t) = 0$  then, by Assumption 1,  $\dot{R}(\xi, \vartheta, t)$  is a continuous function and we have  $\dot{R}(\xi, \vartheta, \tau_f(t)) = 0$ . Therefore, (21) becomes

$$\frac{\partial R(\xi, \vartheta, t)}{\partial b} = \int_{\tau_f}^t \frac{\partial \dot{R}(\xi, \vartheta, \delta)}{\partial b} d\delta \quad (22)$$

where  $\dot{R}(\xi, \vartheta, \delta) = A(\xi, \vartheta) - Bp(\xi, \vartheta, s(\delta))$ .

If, on the other hand,  $\tau_f(t) = t$ , then  $R(\xi, \vartheta, t) = 0$  and we define  $\sigma_f(t) = \sup_{\sigma \leq t} \{ \sigma : R(\xi, \vartheta, \sigma) > 0 \}$ . Proceeding as above, we get

$$\frac{\partial R(\xi, \vartheta, t)}{\partial b} = \int_{\sigma_f}^t \frac{\partial \dot{R}(\xi, \vartheta, \delta)}{\partial b} d\delta$$

where now  $\dot{R}(\xi, \vartheta, \delta) = 0$  and we get

$$\frac{\partial R(\xi, \vartheta, t)}{\partial b} = 0 \quad (23)$$

(ii)  $R(\xi, \vartheta, t') > 0$  for all  $t' \in (0, t)$ . In this case, we define  $\tau_f(t) = 0$  and we have  $R(\xi, \vartheta, t) = R(\xi, \vartheta, 0) + \int_{\tau_f(t)}^t \dot{R}(\xi, \vartheta, \delta) d\delta$ , where  $\dot{R}(\xi, \vartheta, \delta) = A(\xi, \vartheta) - Bp(\xi, \vartheta, s(t))$ . Thus,

$$\begin{aligned} \frac{\partial R(\xi, \vartheta, t)}{\partial b} &= \frac{\partial R(\xi, \vartheta, 0)}{\partial b} + \frac{\partial t}{\partial b} \dot{R}(\xi, \vartheta, t) \\ &+ \int_{\tau_f(t)}^t \frac{\partial \dot{R}(\xi, \vartheta, \delta)}{\partial b} d\delta \end{aligned} \quad (24)$$

Clearly,  $\frac{\partial t}{\partial b} = 0$  and  $\frac{\partial R(\xi, \vartheta, 0)}{\partial b} = 0$ , since  $R(\xi, \vartheta, 0)$  is the initial uncertainty value at  $(\xi, \vartheta)$ . Then, (24) becomes

$$\frac{\partial R(\xi, \vartheta, t)}{\partial b} = \int_{\tau_f}^t \frac{\partial \dot{R}(\xi, \vartheta, \delta)}{\partial b} d\delta \quad (25)$$

which is the same result as (22).

Let us set aside the much simpler case where (23) applies and consider (22) and (25). Noting that  $\frac{\partial A(\xi, \vartheta)}{\partial b} = 0$  we get

$$\frac{\partial \dot{R}(\xi, \vartheta, \delta)}{\partial b} = -B \frac{\partial p(\xi, \vartheta, s(\delta))}{\partial b} \quad (26)$$

Recall that  $[X, Y]$  has been selected to be the origin and that  $\varphi = 0$ . In this case, (12) becomes

$$s^x(t) = a \cos \rho(t), \quad s^y(t) = b \sin \rho(t) \quad (27)$$

Observing that  $s^x(t)$  is independent of  $b$ , (26) gives

$$\begin{aligned} \frac{\partial \dot{R}(\xi, \vartheta, \delta)}{\partial b} &= -B \frac{\partial p(\xi, \vartheta, s(\delta))}{\partial s^y(\delta)} \frac{\partial s^y(\delta)}{\partial b} \\ &= -B \frac{\partial p(\xi, \vartheta, s(\delta))}{\partial D(\xi, \vartheta, s(\delta))} \frac{\partial D(\xi, \vartheta, s(\delta))}{\partial s^y(\delta)} \sin \rho(\delta) \end{aligned} \quad (28)$$

where  $D(\xi, \vartheta, s(\delta)) = [(s^x(\delta) - \xi \cos \vartheta)^2 + (s^y(\delta) - \xi \sin \vartheta)^2]^{1/2}$ , hence

$$\frac{\partial D(\xi, \vartheta, s(\delta))}{\partial s^y(\delta)} = \frac{s^y(\delta) - \xi \sin \vartheta}{D(\xi, \vartheta, s(\delta))} \quad (29)$$

Using (29), (28), (22) in the second integral of (18), this integral becomes

$$\begin{aligned} &\int_0^T \int_0^{2\pi} \int_0^{\gamma(\vartheta)} \frac{\partial R(\xi, \vartheta, t)}{\partial b} \xi d\xi d\vartheta dt \\ &= -B \int_0^T \int_0^{2\pi} \int_0^{\gamma(\vartheta)} \xi \int_{\tau_f}^t \frac{\partial p(\xi, \vartheta, s(\delta))}{\partial D(\xi, \vartheta, s(\delta))} \frac{(s_y(\delta) - \xi \sin \vartheta)}{D(\xi, \vartheta, s(\delta))} \\ &\cdot \sin \rho(\delta) d\delta d\xi d\vartheta dt \end{aligned} \quad (30)$$

Note that when  $b \rightarrow 0$ , we have  $s_y(\delta) \rightarrow 0$ . In addition,  $p(\xi, \vartheta, s(\delta))$  is a direct function of  $D(\xi, \vartheta, s(\delta))$ , so that  $\frac{\partial p(\xi, \vartheta, s(\delta))}{\partial D(\xi, \vartheta, s(\delta))}$  is not an explicit function of  $\xi, \vartheta$  or  $\delta$ . Moreover,  $\sin \rho(\delta)$  is not a function of  $\vartheta$ . Thus, switching the integration order in (30) we get

$$B \frac{\partial p(D)}{\partial D} \int_0^T \int_{\tau_f}^t \sin \rho(\delta) \int_0^{2\pi} \int_0^{\gamma(\vartheta)} \frac{\xi^2 \sin \vartheta}{D(\xi, \vartheta, s(\delta))} d\xi d\vartheta d\delta dt$$

Using Assumption 2, we make a symmetry argument similar to the one regarding (19). For any point  $\omega = (\xi, \vartheta) \in \mathbb{R}^2$ , we can find  $(\xi, \vartheta + \pi)$  which is symmetric to it with respect to the center point of the ellipse and Assumption 2 implies that

$A(\xi, \vartheta) = A(\xi, \vartheta + \pi)$ . Then, from the perspective of the point  $(\xi, \vartheta)$ , the agent movement observed with an initial position  $\rho(0) = \eta$  (following the dynamics in (IV)) is the same as the movement observed from  $(\xi, \vartheta + \pi)$  if the agent starts from  $\rho(0) = \eta + \pi$  when  $T \rightarrow \infty$ , since the cost in (13) is independent of initial conditions as  $T \rightarrow \infty$ . In addition, we again have  $\gamma(\vartheta) = \gamma(\vartheta + \pi)$ , so that  $\int_0^{\gamma(\vartheta)} \frac{\sin \vartheta}{D(\xi, \vartheta, s(\delta))} = -\int_0^{\gamma(\vartheta+\pi)} \frac{\sin(\vartheta+\pi)}{D(\xi, \vartheta+\pi, s(\delta))}$ . Therefore,

$$\lim_{T \rightarrow \infty} \int_0^{2\pi} \int_0^{\gamma(\vartheta)} \frac{\xi^2 \sin \vartheta}{D(\xi, \vartheta, s(\delta))} d\xi d\vartheta = 0 \quad (31)$$

and the second term of (18) gives

$$\lim_{T \rightarrow \infty, b \rightarrow 0} \int_0^T \int_0^{2\pi} \int_0^{\gamma(\vartheta)} \frac{\partial R(\xi, \vartheta, t)}{\partial b} \xi d\xi d\vartheta dt = 0 \quad (32)$$

In view of (19) and (32), we have shown that the second term of (17) is 0 and we are left with the first negative term from (14), giving the desired result:

$$\lim_{T \rightarrow \infty, b \rightarrow 0} \frac{\partial J(b)}{\partial b} = -\frac{\partial \Psi_\Omega}{\partial b} \frac{1}{\Psi_\Omega^2} \int_0^T \int_\Omega R(\omega, t) d\omega dt < 0 \quad (33)$$

Finally, if (23) applies instead of (22), then (23) and (19) immediately imply that the second term of (17) is 0, completing the proof. ■

Thus, we have proved that as  $T \rightarrow \infty$ , when  $b$  is perturbed from 0 to some  $b_\varepsilon > 0$ , an elliptical trajectory achieves a lower cost than a linear one. In other words, we have shown that elliptical trajectories are more suitable for a 2D mission space in terms of achieving near-optimal results in solving problem **P1**.

## V. OPTIMAL ELLIPTICAL TRAJECTORIES

Based on our analysis thus far, our approach is to associate with each agent an elliptical trajectory, parameterize each such trajectory by its center, orientation and major and minor axes, and then solve **P1** as a parametric optimization problem. Note that this includes the possibility that two agents share the same trajectory if the solution to this problem results in identical parameters for the associated ellipses. For an elliptical trajectory, the  $n$ th agent movement is described as in (12) by

$$\begin{cases} s_n^x(t) = X_n + a_n \cos \rho_n(t) \cos \varphi_n - b_n \sin \rho_n(t) \sin \varphi_n \\ s_n^y(t) = Y_n + a_n \cos \rho_n(t) \sin \varphi_n + b_n \sin \rho_n(t) \cos \varphi_n \end{cases} \quad (34)$$

where  $[X_n, Y_n]$  is the center of the  $n$ th ellipse,  $a_n, b_n$  are its major and minor axes respectively and  $\varphi_n \in [0, \pi)$  is its orientation. Note that the parameter  $\rho_n(t) \in [0, 2\pi)$  is the eccentric anomaly. Therefore, we replace problem **P1** by the determination of optimal parameter vectors  $\Upsilon_n \equiv [X_n, Y_n, a_n, b_n, \varphi_n]^T, n = 1, \dots, N$ , and formulate the following problem **P2**:

$$\min_{\Upsilon_n, n=1, \dots, N} J = \int_0^T \sum_{i=1}^M \sum_{n=1}^N R_i(\Upsilon_1, \dots, \Upsilon_N, t) dt \quad (35)$$

We solve this problem using a gradient-based approach in which we apply IPA to determine the gradients

$\nabla R_i(\Upsilon_1, \dots, \Upsilon_N, t)$  on line (hence,  $\nabla J$ ), i.e., directly using information from the agent trajectories and iterate upon them.

**IPA review.** The purpose of IPA [14] is to study the behavior of a hybrid system state as a function of a parameter vector  $\theta \in \Theta$  for a given compact, convex set  $\Theta \subset \mathbb{R}^l$ . Let  $\{\tau_k(\theta)\}, k = 1, \dots, K$ , denote the occurrence times of all events in the state trajectory. For convenience, we set  $\tau_0 = 0$  and  $\tau_{K+1} = T$ . Over an interval  $[\tau_k(\theta), \tau_{k+1}(\theta))$ , the system is at some mode during which the time-driven state satisfies  $\dot{x} = f_k(x, \theta, t)$ . An event at  $\tau_k$  is classified as (i) *Exogenous* if it causes a discrete state transition independent of  $\theta$  and satisfies  $\frac{d\tau_k}{d\theta} = 0$ ; (ii) *Endogenous*, if there exists a continuously differentiable function  $g_k: \mathbb{R}^n \times \Theta \rightarrow \mathbb{R}$  such that  $\tau_k = \min\{t > \tau_{k-1} : g_k(x(\theta, t), \theta) = 0\}$ ; and (iii) *Induced* if it is triggered by the occurrence of another event at time  $\tau_m \leq \tau_k$ . IPA specifies how changes in  $\theta$  influence the state  $x(\theta, t)$  and the event times  $\tau_k(\theta)$  and, ultimately, how they influence interesting performance metrics which are generally expressed in terms of these variables.

We define:  $x'(t) \equiv \frac{\partial x(\theta, t)}{\partial \theta}$ ,  $\tau'_k \equiv \frac{\partial \tau_k(\theta)}{\partial \theta}$ ,  $k = 1, \dots, K$ , for all state and event time derivatives. It is shown in [14] that  $x'(t)$  satisfies:

$$\frac{d}{dt} x'(t) = \frac{\partial f_k(t)}{\partial x} x'(t) + \frac{\partial f_k(t)}{\partial \theta} \quad (36)$$

for  $t \in [\tau_k, \tau_{k+1})$  with boundary condition:

$$x'(\tau_k^+) = x'(\tau_k^-) + [f_{k-1}(\tau_k^-) - f_k(\tau_k^+)] \tau'_k \quad (37)$$

for  $k = 0, \dots, K$ . In addition, in (37), the gradient vector for each  $\tau_k$  is  $\tau'_k = 0$  if the event at  $\tau_k$  is exogenous and

$$\tau'_k = - \left[ \frac{\partial g_k}{\partial x} f_k(\tau_k^-) \right]^{-1} \left( \frac{\partial g_k}{\partial \theta} + \frac{\partial g_k}{\partial x} x'(\tau_k^-) \right) \quad (38)$$

if the event at  $\tau_k$  is endogenous (i.e.,  $g_k(x(\theta, \tau_k), \theta) = 0$ ) and defined as long as  $\frac{\partial g_k}{\partial x} f_k(\tau_k^-) \neq 0$ .

In our case, the parameter vectors are  $\Upsilon_n \equiv [X_n, Y_n, a_n, b_n, \varphi_n]^T, n = 1, \dots, N$  as defined earlier, and we seek to determine optimal vectors  $\Upsilon_n^*$ . We will use IPA to evaluate  $\nabla J(\Upsilon_1, \dots, \Upsilon_N) = [\frac{dJ}{d\Upsilon_1}, \dots, \frac{dJ}{d\Upsilon_N}]^T$ . From (35), this gradient clearly depends on  $\nabla R_i(t) = [\frac{\partial R_i(t)}{\partial \Upsilon_1}, \dots, \frac{\partial R_i(t)}{\partial \Upsilon_N}]^T$ . In turn, this gradient depends on whether the dynamics of  $R_i(t)$  in (3) are given by  $\dot{R}_i(t) = 0$  or  $\dot{R}_i(t) = A_i - BP_i(s(t))$ . The dynamics switch at event times  $\tau_k, k = 1, \dots, K$ , when  $R_i(t)$  reaches or escapes from 0 which are observed on a trajectory over  $[0, T]$  based on a given  $\Upsilon_n, n = 1, \dots, N$ .

**IPA equations.** We begin by recalling the dynamics of  $R_i(t)$  in (3) which depend on the relative positions of all agents with respect to  $[\alpha_i, \beta_i]$  and change at time instants  $\tau_k$  such that either  $R_i(\tau_k) = 0$  with  $R_i(\tau_k^-) > 0$  or  $A_i > BP_i(s(\tau_k))$  with  $R_i(\tau_k^-) = 0$ . Moreover, the agent positions  $s_n(t) = [s_n^x(t), s_n^y(t)], n = 1, \dots, N$ , on an elliptical trajectory are expressed using (34). Viewed as a hybrid system, we can now concentrate on all events causing transitions in the dynamics of  $R_i(t), i = 1, \dots, M$ , since any other event has no effect on the values of  $\nabla R_i(\Upsilon_1, \dots, \Upsilon_N, t)$  at  $t = \tau_k$ .

For notational simplicity, we define  $\omega_i = [\alpha_i, \beta_i] \in \Omega$ . First, if  $R_i(t) = 0$  and  $A(\omega_i) - BP(\omega_i, s(t)) < 0$ , applying (36) to

$R_i(t)$  and using (3) gives  $\frac{d}{dt} \frac{\partial R_i(t)}{\partial Y_n} = 0$ . When  $R_i(t) > 0$ , we have

$$\frac{d}{dt} \frac{\partial R_i(t)}{\partial Y_n} = -B \frac{\partial p_n(\omega_i, s_n(t))}{\partial Y_n} \prod_{d \neq n} [1 - p_d(\omega_i, s_d(t))] \quad (39)$$

Adopting the sensing model (2) and noting that  $p_n(\omega_i, s_n(t)) \equiv p_n(D(\omega_i, s_n(t)))$ ,  $D(\omega_i, s_n(t)) = [(s_n(t)^x - \alpha_i)^2 + (s_n(t)^y - \beta_i)^2]^{1/2}$  we get

$$\frac{\partial p_n(\omega_i, s_n(t))}{\partial Y_n} = \frac{-1}{2Dr_n} \left( \frac{\partial D}{\partial s_n^x} \frac{\partial s_n^x}{\partial Y_n} + \frac{\partial D}{\partial s_n^y} \frac{\partial s_n^y}{\partial Y_n} \right) \quad (40)$$

where  $\frac{\partial D}{\partial s_n^x} = 2(s_n^x - \alpha_i)$  and  $\frac{\partial D}{\partial s_n^y} = 2(s_n^y - \beta_i)$ . Note that  $\frac{\partial s_n^x}{\partial Y_n} = [\frac{\partial s_n^x}{\partial X_n}, \frac{\partial s_n^x}{\partial Y_n}, \frac{\partial s_n^x}{\partial a_n}, \frac{\partial s_n^x}{\partial b_n}, \frac{\partial s_n^x}{\partial \varphi_n}]^T$  and  $\frac{\partial s_n^y}{\partial Y_n} = [\frac{\partial s_n^y}{\partial X_n}, \frac{\partial s_n^y}{\partial Y_n}, \frac{\partial s_n^y}{\partial a_n}, \frac{\partial s_n^y}{\partial b_n}, \frac{\partial s_n^y}{\partial \varphi_n}]^T$ . From (34), for  $\frac{\partial s_n^x}{\partial Y_n}$ , we obtain  $\frac{\partial s_n^x}{\partial X_n} = 1$ ,  $\frac{\partial s_n^x}{\partial Y_n} = 0$ ,  $\frac{\partial s_n^x}{\partial a_n} = \cos \rho_n(t) \cos \varphi_n$ ,  $\frac{\partial s_n^x}{\partial b_n} = -\sin \rho_n(t) \sin \varphi_n$  and  $\frac{\partial s_n^x}{\partial \varphi_n} = -a_n \cos \rho_n(t) \sin \varphi_n - b_n \sin \rho_n(t) \cos \varphi_n$ . Similarly, for  $\frac{\partial s_n^y}{\partial Y_n}$ , we get  $\frac{\partial s_n^y}{\partial X_n} = 0$ ,  $\frac{\partial s_n^y}{\partial Y_n} = 1$ ,  $\frac{\partial s_n^y}{\partial a_n} = \cos \rho_n(t) \sin \varphi_n$ ,  $\frac{\partial s_n^y}{\partial b_n} = \sin \rho_n(t) \cos \varphi_n$  and  $\frac{\partial s_n^y}{\partial \varphi_n} = a_n \cos \rho_n(t) \cos \varphi_n - b_n \sin \rho_n(t) \sin \varphi_n$ . Using  $\frac{\partial s_n^x}{\partial Y_n}$  and  $\frac{\partial s_n^y}{\partial Y_n}$  in (40) and then (??) and back into (39), we can finally obtain  $\frac{\partial R_i(t)}{\partial Y_n}$  for  $t \in [\tau_k, \tau_{k+1})$  as

$$\frac{\partial R_i(t)}{\partial Y_n} = \frac{\partial R_i(\tau_k^+)}{\partial Y_n} + \begin{cases} 0 & \text{if } R_i(t) = 0, \\ A_i < BP_i(\mathbf{s}(t)) & \\ \int_{\tau_k}^t \frac{d}{dt} \frac{\partial R_i(t)}{\partial Y_n} dt & \text{otherwise} \end{cases} \quad (41)$$

Thus, it remains to determine the components  $\nabla R_i(\tau_k^+)$  in (41) using (37). This involves the event time gradient vectors  $\nabla \tau_k = \frac{\partial \tau_k}{\partial Y_n}$  for  $k = 1, \dots, K$ , which will be determined through (38). There are two possible cases regarding the events that cause switches in the dynamics of  $R_i(t)$ :

*Case 1:* At  $\tau_k$ ,  $\dot{R}_i(t)$  switches from  $\dot{R}_i(t) = 0$  to  $\dot{R}_i(t) = A_i - BP_i(\mathbf{s}(t))$ . In this case, it is easy to see that the dynamics  $R_i(t)$  are continuous, so that  $f_{k-1}(\tau_k^-) = f_k(\tau_k^+)$  in (37) applied to  $R_i(t)$  and we get

$$\nabla R_i(\tau_k^+) = \nabla R_i(\tau_k^-), \quad i = 1, \dots, M \quad (42)$$

*Case 2:* At  $\tau_k$ ,  $\dot{R}_i(t)$  switches from  $\dot{R}_i(t) = A_i - BP_i(\mathbf{s}(t))$  to  $\dot{R}_i(t) = 0$ , i.e.,  $R_i(\tau_k)$  becomes zero. In this case, we need to first evaluate  $\nabla \tau_k$  from (38) in order to determine  $\nabla R_i(\tau_k^+)$  through (37). Observing that this event is endogenous, (38) applies with  $g_k = R_i = 0$  and we get  $\nabla \tau_k = -\frac{\nabla R_i(\tau_k^-)}{A(\omega_i) - BP(\omega_i, \mathbf{s}(\tau_k^-))}$ . It follows from (37) that

$$\nabla R_i(\tau_k^+) = \nabla R_i(\tau_k^-) - \frac{[A(\omega_i) - BP(\omega_i, \mathbf{s}(\tau_k^-))] \nabla R_i(\tau_k^-)}{A(\omega_i) - BP(\omega_i, \mathbf{s}(\tau_k^-))} = 0 \quad (43)$$

Thus,  $\nabla R_i(\tau_k^+)$  is always reset to 0 regardless of  $\nabla R_i(\tau_k^-)$ .

**Objective Function Gradient Evaluation.** Based on our analysis, we first rewrite  $J$  in (35) as

$$J(Y_1, \dots, Y_N) = \sum_{i=1}^M \sum_{k=0}^K \int_{\tau_k(Y_1, \dots, Y_N)}^{\tau_{k+1}(Y_1, \dots, Y_N)} R_i(t, Y_1, \dots, Y_N) dt$$

and (omitting some function arguments) we get

$$\nabla J = \sum_{i=1}^M \sum_{k=0}^K \left( \int_{\tau_k}^{\tau_{k+1}} \nabla R_i(t) dt + R_i(\tau_{k+1}) \nabla \tau_{k+1} - R_i(\tau_k) \nabla \tau_k \right)$$

Observing the cancelation of all terms of the form  $R_i(\tau_k) \nabla \tau_k$  for all  $k$  (with  $\tau_0 = 0$ ,  $\tau_{K+1} = T$  fixed), we finally get

$$\nabla J(Y_1, \dots, Y_N) = \frac{1}{T} \sum_{i=1}^M \sum_{k=0}^K \int_{\tau_k}^{\tau_{k+1}} \nabla R_i(t) dt$$

This depends entirely on  $\nabla R_i(t)$ , which is obtained from (41) and the event times  $\tau_k$ ,  $k = 1, \dots, K$ , given initial conditions  $s_n(0)$  for  $n = 1, \dots, N$ , and  $R_i(0)$  for  $i = 1, \dots, M$ . In (41),  $\frac{\partial R_i(\tau_k^+)}{\partial Y_n}$  is obtained through (42)-(43), whereas  $\frac{d}{dt} \frac{\partial R_i(t)}{\partial Y_n}$  is obtained through (39)-(40). Note that this approach is scalable in the number of events where any  $R_i(t)$  switches dynamics.

**Objective Function Optimization.** We now seek to obtain  $[Y_1^*, \dots, Y_N^*]$  minimizing  $J(Y_1, \dots, Y_N)$  through a standard gradient-based optimization algorithm of the form

$$[Y_1^{l+1}, \dots, Y_N^{l+1}] = [Y_1^l, \dots, Y_N^l] - [\alpha_1^l, \dots, \alpha_N^l] \tilde{\nabla} J(Y_1, \dots, Y_N) \quad (44)$$

where  $\{\alpha_n^l\}$ ,  $l = 1, 2, \dots$  are appropriate step size sequences and  $\tilde{\nabla} J(Y_1, \dots, Y_N)$  is the projection of the gradient  $\nabla J(Y_1, \dots, Y_N)$  onto the feasible set, i.e.,  $s_n(t) \in \Omega$  for all  $n$ ,  $t \in [0, T]$ . The algorithm terminates when  $|\tilde{\nabla} J(Y_1, \dots, Y_N)| < \varepsilon$  (for a fixed threshold  $\varepsilon$ ) for some  $[Y_1^*, \dots, Y_N^*]$ .

## VI. NUMERICAL RESULTS

A two-agent example of solving **P1** using a TPBVP solver is shown in Fig. 2. The same two-agent example solving **P2** with optimal elliptical trajectories is shown in Fig. 3. In both cases the same environment settings are used:  $r = 4$ ,  $L_1 = 20$ ,  $L_2 = 10$ ,  $T = 200$ . All sampling points  $[\alpha_i, \beta_i]$  are uniformly spaced within  $L_1 \times L_2$ ,  $i = 1, \dots, M$ . Note that  $M = (L_1 + 1)(L_2 + 1) = 231$ . Initial values are  $R_i(0) = 2$  and  $B = 6$ ,  $A_i = 0.2$  for all  $i = 1, \dots, M$ .

In Fig. 2, the top plot shows the two agent initial trajectories assigned to the environment, while the bottom plot shows the trajectories that the TPBVP solver converges to. The optimal cost is  $J^* = 5.74 \times 10^4$ . In Fig. 3, the red ellipses are the ones we initially selected (with random location and orientation) and the blue ellipses are the ones resulting when (44) converges. We deliberately choose  $b$  to be very small, approximating linear trajectories, in order to illustrate Proposition IV.1: we can see that larger ellipses achieve a lower total uncertainty value per unit area. Note that the initial cost is significantly reduced indicating the importance of optimally selecting the ellipse sizes, locations and orientations. The corresponding cost in this case is  $J_e = 6.45 \times 10^4$ , which is not much higher than the TPBVP result above, as expected. Moreover, if we replace the rectangular mission space  $\Omega$  by an ellipsoidal one (of slightly larger size), then we find that  $J_e = 1.44 \times 10^5$  compared to the (locally) optimal cost from a TPBVP solver  $J^* = 1.32 \times 10^5$ , a much smaller difference.

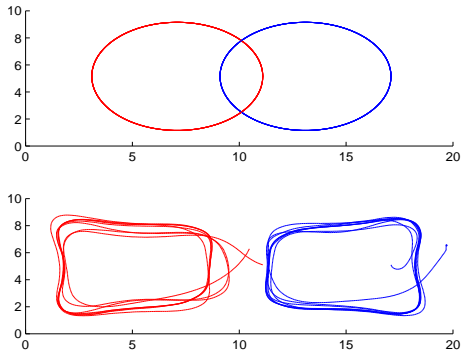


Fig. 2. Top: initially assigned trajectories for two agents. Bottom: trajectories obtained by solving associated TPBVP. Optimal cost:  $J^* = 5.74 \times 10^4$ .

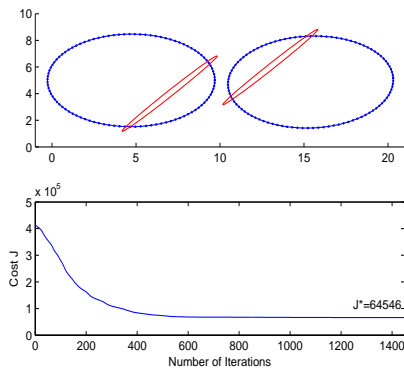


Fig. 3. Red ellipses: initial randomly selected elliptical trajectories. Blue ellipses: trajectories obtained solving problem **P2**.  $J_e = 6.45 \times 10^4$ .

## VII. CONCLUSION

We have shown that an optimal control solution to the 1D persistent monitoring problem does not easily extend to the 2D case. In particular, we have proved that elliptical trajectories outperform linear ones in a 2D mission space. Therefore, we have sought to solve a parametric optimization problem to determine optimal elliptical trajectories. Numerical examples indicate that this scalable approach (which can be used on line) provides solutions that approximate those obtained through a computationally intensive TPBVP solver. Ongoing work aims at alternative approaches for near-optimal solutions and at distributed implementations.

## REFERENCES

- [1] M. Zhong and C. G. Cassandras, "Distributed coverage control and data collection with mobile sensor networks," *Automatic Control, IEEE Transactions on*, vol. 56, no. 10, pp. 2445–2455, 2011.
- [2] J. Cortes, S. Martinez, T. Karatas, and F. Bullo, "Coverage control for mobile sensing networks," *IEEE Trans. on Robotics and Automation*, vol. 20, no. 2, pp. 243–255, 2004.
- [3] B. Grocholsky, J. Keller, V. Kumar, and G. Pappas, "Cooperative air and ground surveillance," *IEEE Robotics & Automation Magazine*, vol. 13, no. 3, pp. 16–25, 2006.
- [4] R. Smith, S. Mac Schwager, D. Rus, and G. Sukhatme, "Persistent ocean monitoring with underwater gliders: Towards accurate reconstruction of dynamic ocean processes," in *IEEE Conf. on Robotics and Automation*, 2011, pp. 1517–1524.

- [5] D. Paley, F. Zhang, and N. Leonard, "Cooperative control for ocean sampling: The glider coordinated control system," *IEEE Trans. on Control Systems Technology*, vol. 16, no. 4, pp. 735–744, 2008.
- [6] P. Dames, M. Schwager, V. Kumar, and D. Rus, "A decentralized control policy for adaptive information gathering in hazardous environments," in *51st IEEE Conf. Decision and Control*, 2012, pp. 2807–2813.
- [7] S. L. Smith, M. Schwager, and D. Rus, "Persistent monitoring of changing environments using robots with limited range sensing," *IEEE Trans. on Robotics*, 2011.
- [8] N. Nigam and I. Kroo, "Persistent surveillance using multiple unmanned air vehicles," in *IEEE Aerospace Conf.*, 2008, pp. 1–14.
- [9] P. Hokayem, D. Stipanovic, and M. Spong, "On persistent coverage control," in *46th IEEE Conf. Decision and Control*, 2008, pp. 6130–6135.
- [10] B. Julian, M. Angermann, and D. Rus, "Non-parametric inference and coordination for distributed robotics," in *51st IEEE Conf. Decision and Control*, 2012, pp. 2787–2794.
- [11] Y. Chen, K. Deng, and C. Belta, "Multi-agent persistent monitoring in stochastic environments with temporal logic constraints," in *51st IEEE Conf. Decision and Control*, 2012, pp. 2801–2806.
- [12] C. G. Cassandras, X. C. Ding, and X. Lin, "An optimal control approach for the persistent monitoring problem," in *Proc. of 50th IEEE Conf. Decision and Control*, 2011, pp. 2907–2912.
- [13] C. G. Cassandras, X. Lin, and X. C. Ding, "An optimal control approach to the multi-agent persistent monitoring problem," *IEEE Trans. on Automatic Control*, vol. 58, no. 4, pp. 947–961, 2013.
- [14] C. G. Cassandras, Y. Wardi, C. G. Panayiotou, and C. Yao, "Perturbation analysis and optimization of stochastic hybrid systems," *European Journal of Control*, vol. 16, no. 6, pp. 642–664, 2010.